

## DEVELOPMENT OF CLOUD DETECTION METHOD FOR CAS500-1 IMAGERY

W. W. Seo<sup>1</sup>, W. S. Yoon<sup>1</sup>, H. Kang<sup>1</sup>, P. C. Lim<sup>1</sup>, T. Kim<sup>2\*</sup>

<sup>1</sup> Image Engineering Research Centre, 3D Labs Co. Ltd, 56 Songdogwahak-ro, Republic of Korea  
(winter0233, wsyoon, khonchi, lpc314)@3dlabs.co.kr

<sup>2</sup> Dept. of Geoinformatic Engineering, Inha University, 100 Inha-ro, Republic of Korea – tezyd@inha.ac.kr

**KEY WORDS:** CAS500-1, Cloud detection, HSV, Triangle thresholding, Maximum likelihood

### ABSTRACT:

Clouds are typically characterized by high reflectance and low brightness temperature. They are generally classified as noise in optical land monitoring satellites. In particular, the presence of clouds has a decisive effect on the quality of follow-up data, so they must be detected. In this study, pre-processing was applied to effectively detect clouds while minimizing noise using CAS500-1 images with visible and near-infrared bands. First, the RGB color space is converted to the HSV color space. Next, a triangle thresholding method is applied to the value channel, which exhibits the highest correlation with pixel brightness, to extract bright objects. Then, the maximum likelihood method is applied to differentiate between bright objects and cloud candidate objects. Finally, threshold values for cloud detection are automatically determined to create initial cloud maps using the statistical values derived from the cloud candidate objects. We compared the results generated by the single thresholding method to verify the performance of the proposed method. As a result, the proposed method was able to detect clouds more accurately by considering the reflectance characteristics of each image. Moreover, except for cloud objects, the rest of the bright objects (white roofs, concrete roads, sand, etc.) were minimized. Our experiments showed high stability despite the absence of shortwave infrared and thermal infrared bands, which are effective for cloud detection.

### 1. INTRODUCTION

The Compact Advanced Satellite 500 (CAS500) program has started by Korean Government for promoting the space industry and utilization of satellite images. Its first satellite, CAS500-1, has been launched successfully on March 22, 2021.

CAS500-1 provides panchromatic images at a spatial resolution of 0.5m and multispectral images in blue, green, red and near-infrared (NIR) bands at a spatial resolution of 2.0m. In 2025, CAS500-2, with the same specifications, will be launched, and planned to operate with CAS500-1 simultaneously. The National Geographic Information Institute (NGII) is currently developing technology to provide user-friendly image products for CAS500-1 and 2. The products will include surface reflectance and pixel metadata such as cloud, water, no data, missing data, saturation data, and usable data masks.

Clouds are typically characterized by high reflectance and low brightness temperature and are generally classified as noise in optical land monitoring satellites. In particular, the presence of clouds has a decisive effect on the quality of follow-up data, so they must be detected and screened out. For this reason, many studies are being conducted to detect and remove clouds.

Cloud detection technology is divided into a method using a single (or multiple) threshold and a method using multi-temporal images.

The first method is a method of detecting clouds using a specific reflectance or reflectance ratio threshold (Kim and Eun, 2021; Zhong et al., 2017). This can be applied simply and quickly. However, if a single threshold value is applied to multiple images, the deviation of cloud detection accuracy can be severe. In addition, if there is no thermal infrared band effective for cloud detection, cloud detection performance may be lowered.

The second method is a method of detecting clouds using multi-view images based on satellite images with fast observation periods (Lee et al., 2015; Lyapustin et al., 2008). This method assumes that the reflectance of the ground surface does not change within a short period, and if the reflectance increases rapidly, it is regarded as a cloud. However, this method is difficult to apply to satellites with a relatively long revisit period, such as land satellite images.

Cloud detection methods that can be applied to CAS500-1 imagery prefer the method of applying a simple threshold to reflectance in the visible and near-infrared wavelength regions. However, the cloud detection method using a simple threshold value shows very sensitive cloud detection results according to the threshold value. Since there is variation in surface reflectance depending on the time, solar and sensor angle conditions, etc., the simple threshold value method can cause significant errors in cloud detection results. To minimize these problems, recently, deep learning models based on convolutional neural networks (CNN) have been proposed for cloud detection (Guo et al., 2018; Hasan et al., 2022). However, there are difficulties in securing a large amount of training data with a high level of reliability, in particular, for images from a newly launched satellite.

This study proposes pre-processing to effectively detect clouds while minimizing noise using CAS500-1 images with visible and near-infrared bands. The pre-processing performs the conversion of Red-Green-Blue (RGB) color space to Hue-Saturation-Value (HSV) space. Then, it goes through the process of extracting cloud candidate pixels using the value channel that has the greatest correlation with clouds. Cloud candidate pixels extracted through pre-processing are then used as the basis for selecting an automatic threshold.

\* Corresponding author

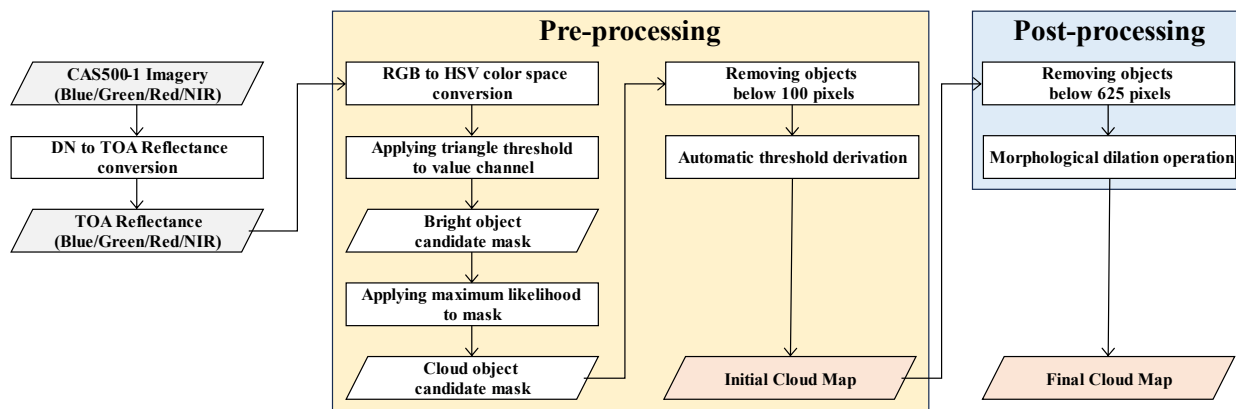


Figure 1. Flowchart of the proposed method

## 2. METHODS

Figure 1 depicts the flowchart illustrating the methodology proposed in this study for cloud detection. First, the RGB color space is converted to the HSV color space. Next, the triangle thresholding method is applied to the value channel, which exhibits the highest correlation with pixel brightness, to extract bright objects. Then, the maximum likelihood method is applied to differentiate between bright objects and cloud candidate objects. Finally, threshold values for cloud detection are automatically determined to create initial cloud maps using the statistical values derived from the cloud candidate objects and finish with post-processing.

### 2.1 Top of atmosphere reflectance conversion

Top-of-atmosphere reflectance (called as TOA reflectance) is the reflectance measured by a space-based sensor flying higher than the Earth's atmosphere. These reflectance values will include contributions from clouds and atmospheric aerosols and gases. Conversion of DN (digital number) to TOA reflectance was applied to clarify the difference in absolute values between the clouds and other surface objects. To convert from DN to TOA Reflectance, there are two processes as shown in Equation (1) and (2).

$$L_{\lambda} = DN * Gain + Offset \quad (1)$$

$$\rho_{\lambda} = \frac{\pi \times L_{\lambda} \times d^2}{ESUN_{\lambda} \times \cos\theta_s} \quad (2)$$

where,

- DN = Digital Number
- $L_{\lambda}$  = TOA Radiance
- $\rho_{\lambda}$  = TOA Reflectance
- d = Earth-Sun distance in astronomical unit
- $ESUN_{\lambda}$  = Mean solar exo-atmospheric irradiance
- $\theta_s$  = Solar Zenith Angle.

### 2.2 RGB to HSV conversion

Clouds represent relatively bright signal values within satellite imagery. Therefore, to identify these bright areas, we convert the blue, green, and red bands of CAS500-1 images to the HSV color space (Figure 2). The HSV color space is a cylindrical coordinate system that arranges colors based on their hue, saturation, and value. By using HSV colors, we can simplify the process of determining the threshold for brightness in the image. Instead of finding a threshold for each of the three-color bands, we set a threshold value for brightness alone. This enables us to identify

cloud cover and other bright features more accurately in the image. The proposed method does not use fixed thresholds on TOA reflectance values, which may change severely due to atmospheric conditions and on-board front-end electronics. This offers robustness to cloud detection.

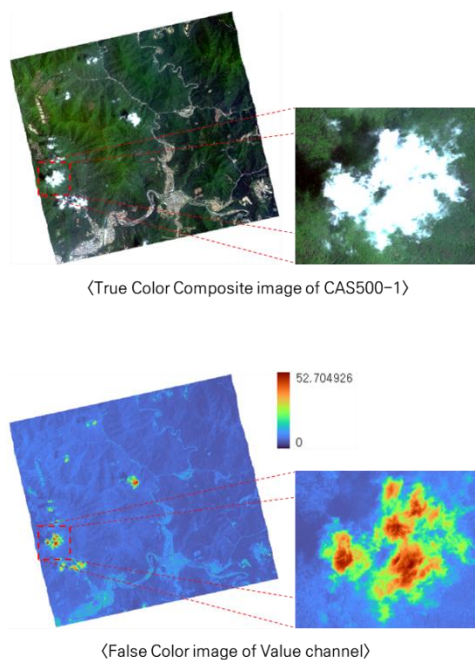


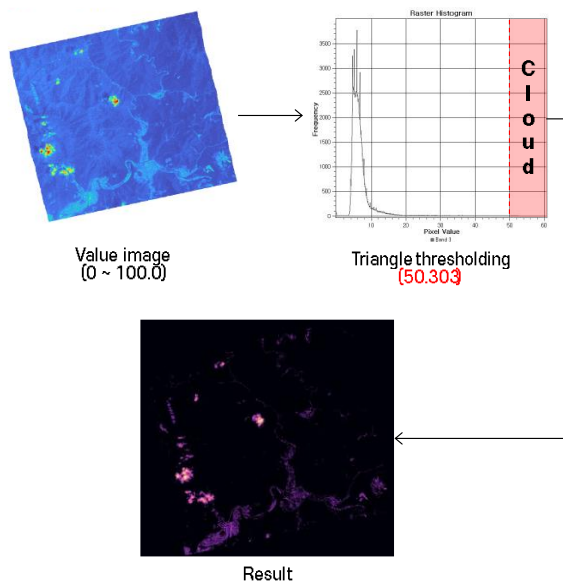
Figure 2. Example of value channel image using true composite image of CAS500-1

### 2.3 Triangle thresholding

Triangle thresholding method is a widely used approach to determine thresholds in images with a maximum frequency peak in one dominant background.

First, a line segment (hereinafter referred to as baseline) connecting the peak of the histogram and the non-zero bin farthest from the peak is calculated. After that, the distance between the baseline and the current bin is calculated at each point in the search interval (peak, base), and the point at which the distance is maximum within the interval is set as the threshold (Zack et al., 1977).

This method was used to separate bright and dark objects in the value channel image (Figure 3).



**Figure 3.** Example of applying the triangle thresholding method

#### 2.4 Maximum likelihood classification

The maximum likelihood method is widely used for classification in remote sensing. In this method, a pixel is assigned to the corresponding class based on its maximum likelihood (Sisodia et al., 2014). It is recognized as a more robust approach compared to Otsu's method, which is commonly used for automatic threshold selection in bimodal distributions with unequal class sizes. The maximum likelihood procedure follows these steps; (1) Assume that the given histogram represents a Gaussian Mixture Model for the two classes. (2) Calculate the mean ( $\mu$ ,  $\nu$ ) and standard deviation ( $\delta$ ,  $\tau$ ) of the two classes using the initial threshold ( $t_0$ ) that separates them. (3) Iteratively calculate the mean ( $\mu$ ,  $\nu$ ) and standard deviation ( $\delta$ ,  $\tau$ ) until they converge using the provided formula. (4) Select the threshold value where the likelihood of between-class variance is maximized.

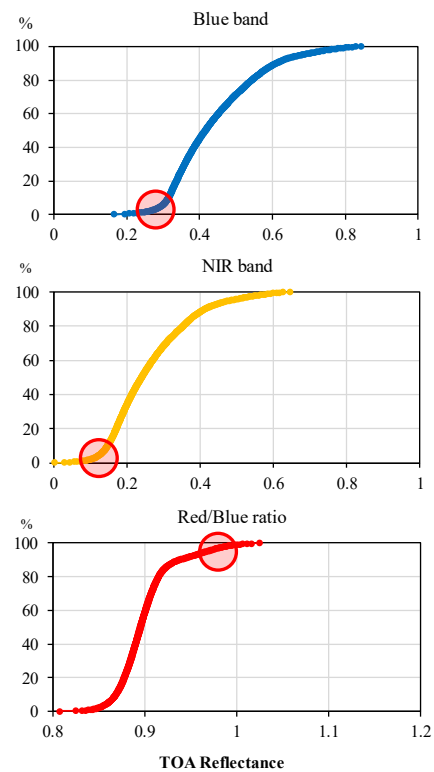
This threshold value is then used to separate the cloud candidate objects from the rest of the bright (or noise) objects.

#### 2.5 Automatic threshold derivation for initial cloud map

An initial cloud map was created using two methods; (1) calculating the mean and standard deviation of cloud candidate objects and (2) utilizing the cumulative distribution function (CDF) of cloud candidate objects.

In the process of applying the first method, the optimal standard deviation coefficient for each band was derived through repeated experiments, and the coefficient was applied to the blue, NIR band, and red/blue ratio suitable for cloud detection. In the second method, Blue, NIR, and Red/Blue ratios were used. The x-axis of the CDF represents the TOA reflectance and the y-axis represents the cumulative probability (Figure 4). The inflection point in the CDF for each band was adopted as the threshold value, and the inflection point at the back of the red/blue ratio graph was adopted as the threshold value.

Among the two results, the cloud map most similar to the cloud candidate pixel extracted through pre-processing was determined as the initial cloud map.



**Figure 4.** Example of threshold estimation method using CDF

#### 2.6 Post-Processing

We applied two post-processing methods to refine the initial cloud map. First, objects smaller than 625 pixels in size were removed to eliminate remaining small noise. Then, we applied morphological dilation operations to compensate for the outer part of the clouds and fill the empty space inside.

#### 2.7 Accuracy Assessment

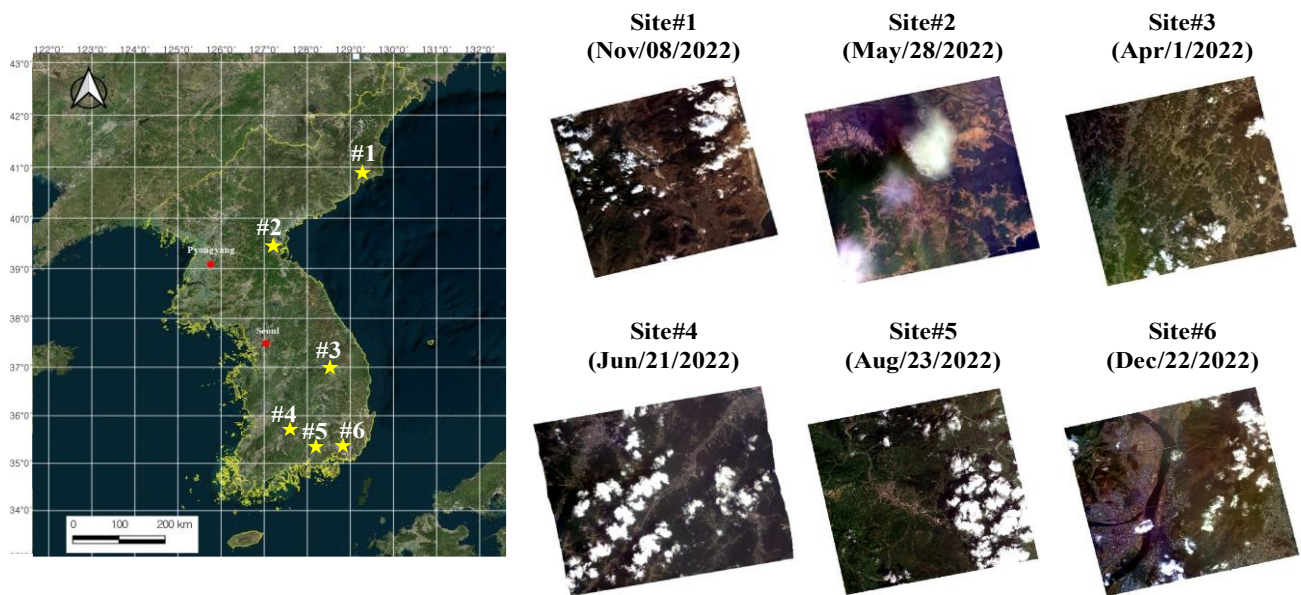
We performed an accuracy assessment on test results. The output is a binary mask consisting of 0 (non-Cloud) and 1 (Cloud). The performance of the detection was evaluated by calculating metrics such as Recall, Precision, and F1-score, which are commonly used for evaluating classification and detection models based on the confusion matrix. Each formula is as follows (equation 3, 4, 5).

A prediction was considered correct when the manually created ground truth (actual values) and the output pixel (predicted values) showed the same value.

$$Recall = \frac{True\ Positive}{True\ Positive + False\ Negative} \quad (3)$$

$$Precision = \frac{True\ Positive}{True\ Positive + False\ Positive} \quad (4)$$

$$F1\ Score = \frac{2 \times Precision \times Recall}{Precision + Recall} \quad (5)$$



**Figure 5.** Study area overview: 6 study area in Korea Peninsula

### 3. MATERIALS

In this experiment, we used images taken by the CAS500-1 satellite from 6 study areas (Figure 5). The images have a spatial resolution of 2.0m and consist of 4 spectral bands: blue, green, red, and NIR. The processing level corresponds to Level-2G (L2G), which precision geometric correction and orthorectification were applied. These images were acquired between April 2022 and December 2022.

### 4. RESULTS AND DISCUSSION

We compared the results of the proposed method with those obtained using simple thresholds applied to multi-temporal images (called as single thresholding method). The quantitative results for the 6 images are shown in Table 1, and the qualitative results are shown in Tables 2 and 3.

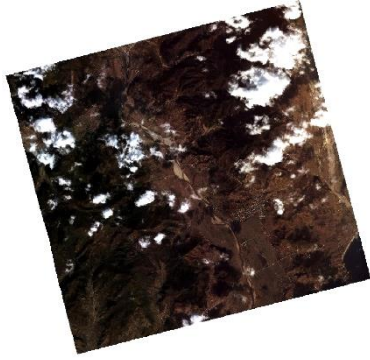
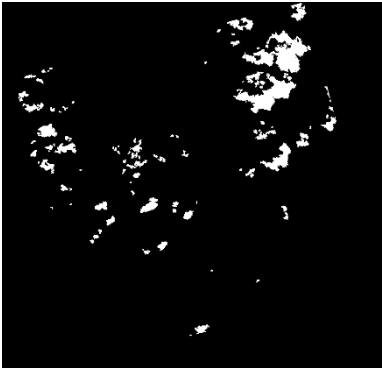
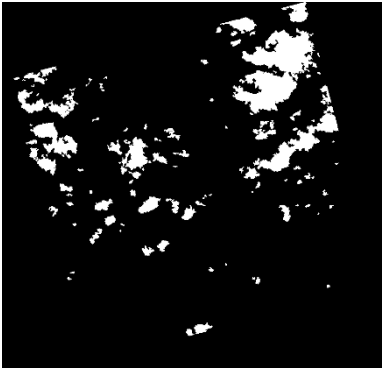




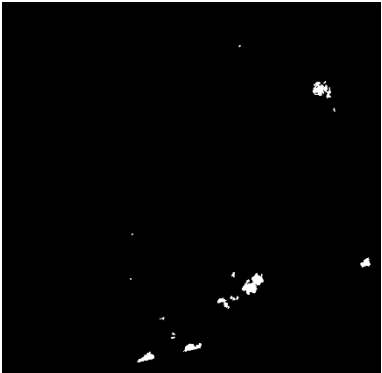
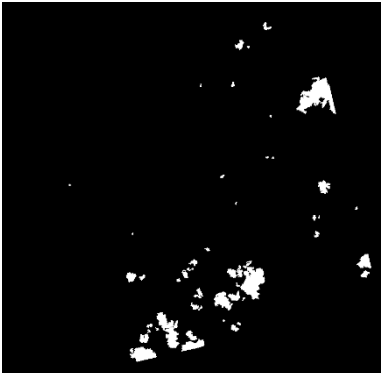

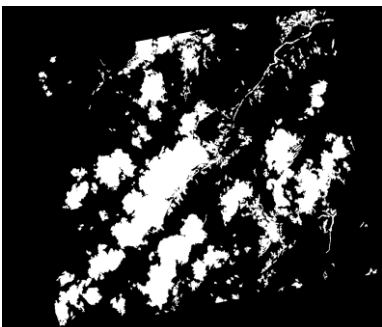
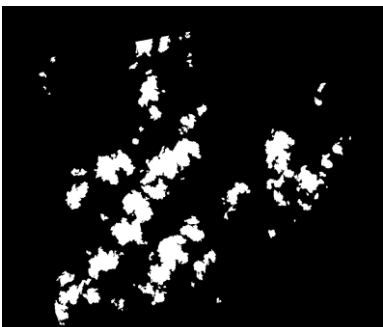
The proposed method exhibited numerous improvements when compared to the single thresholding results. In particular, it effectively reduced noise associated with clouds, as observed in Table 3.

The single thresholding method exhibited a relatively high rate of non-detection due to the lower reflectance typically observed in the outer parts of clouds compared to their centers. Moreover, it showed notable errors in the results, primarily attributed to challenges in considering for variations in reflectance resulting from factors such as different illumination conditions for each image and surrounding environmental influences. In contrast, the proposed method leverages statistical values derived from cloud candidate pixels extracted from each image, enabling it to effectively consider reflectance variation.

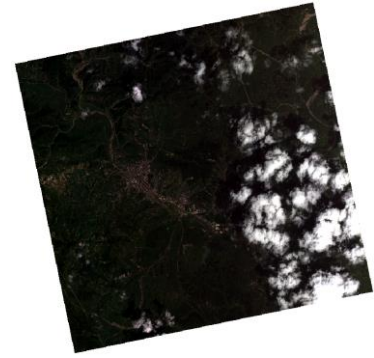
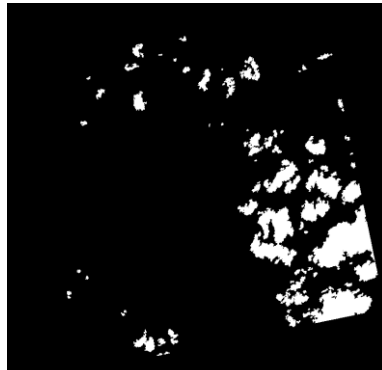
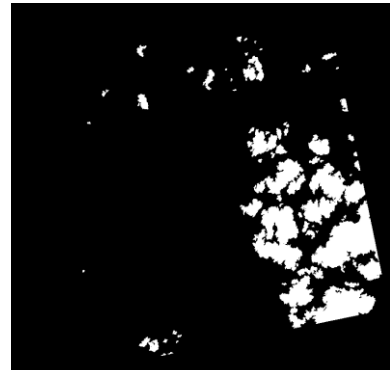
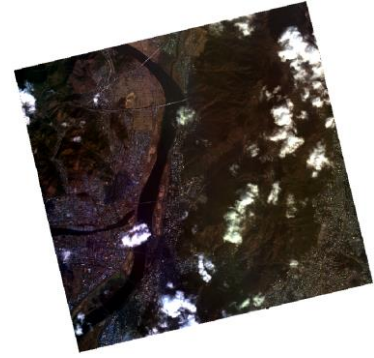
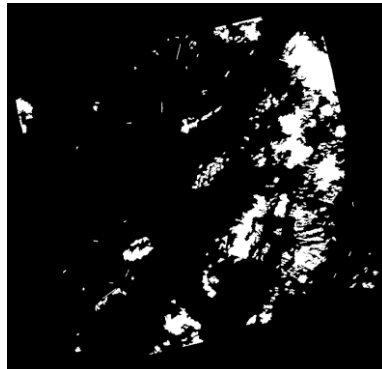
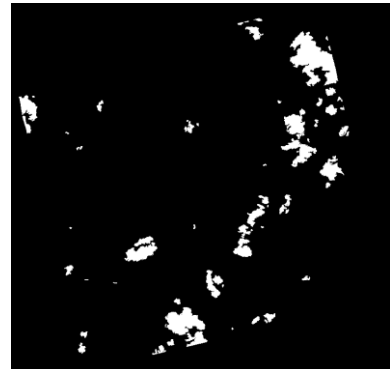
However, some inconsistencies with the ground truth were identified with the proposed method. These inconsistencies included errors where bright ground objects were mistakenly identified as clouds. They occurred when clouds exhibited similar reflectance, posing difficulties in differentiation. Furthermore, the threshold value derived from cloud candidate pixels tended to have lower recall compared to precision. This is because our method prioritizes maximizing cloud detection while potentially minimizing the detection of other objects. In this process, relatively thin clouds such as haze and mist tended to go undetected. It appears that adjusting the offset in the process of applying triangle thresholding could overcome these issues.

Dataset	Single thresholding method			Proposed method		
	Recall	Precision	F1-Score	Recall	Precision	F1-Score
#1	48.6	99.6	65.3	94.5	94.3	94.4
#2	94.9	21.2	34.7	97.6	81.7	88.9
#3	21.8	98.3	35.7	92.4	93.6	93.0
#4	98.1	56.0	71.3	85.6	99.3	91.9
#5	62.0	98.6	76.1	77.1	99.5	86.9
#6	83.5	61.1	70.6	68.6	99.0	81.1

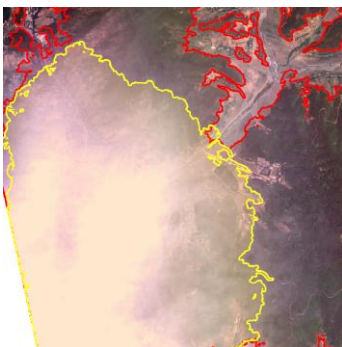

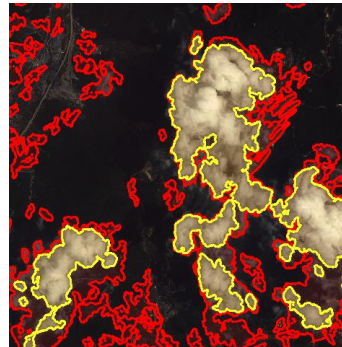


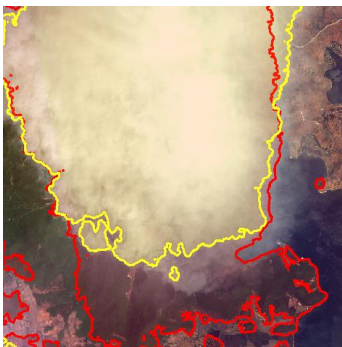
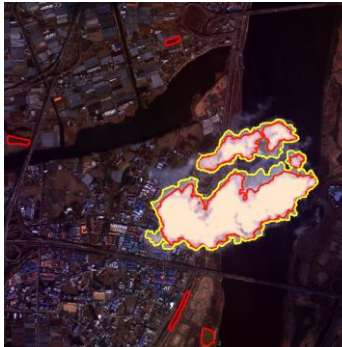
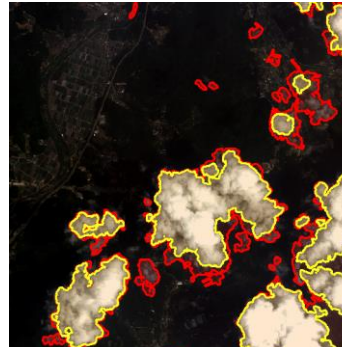
**Table 1.** The accuracy assessment results for Single thresholding method and proposed method

Site	RGB Color Composite	Single thresholding method	Proposed method
#1			
#2			
#3			
#4			

**Table 2.** Cloud detection result using single thresholding and proposed method

Site	RGB Color Composite	Single thresholding method	Proposed method
#5			
#6			

**Table 3.** Cloud detection result using single thresholding and proposed method (cont.)

Site #2	Site #4	Site #6	Legend
			 Single thresholding method  Proposed method
			

**Table 4.** Final cloud maps using the Proposed method compared to the single thresholding cloud maps

## 5. CONCLUSIONS

In this paper, we have presented a new cloud detection method for CAS500-1 images. This method selects the cloud candidate objects in the image through pre-processing and automatically derives the optimal threshold through statistic of pixels included in the object. An initial cloud map is then created and post-processing is applied to create the final cloud map. Our experiments showed high stability despite the absence of shortwave infrared and thermal infrared bands that are effective for cloud detection.

Compared to the single thresholding method, the pre-processing successfully removed noise pixels and detected most of the cloud pixels. Despite the different reflectance variation characteristics for each image, the result was overcome.

However, the quality of the final cloud map was somewhat dependent on the pre-processing result. As a future experiment, we plan to stabilize the pre-processing and the automatic threshold derivation method and to utilize shape index and texture.

## ACKNOWLEDGEMENTS

This work is funded by the National Geographic Information Institute, Republic of Korea, "Surface reflectance and side information product package SW development for CAS500-1" R&D project and National Institute of Agricultural Sciences, Rural Development Administration, Republic of Korea, "Research Program for Agricultural Science & Technology Development (Project No. PJ0162342023)"

## REFERENCES

- Guo, Z., Li, C., Wang, Z., Kwok, E., Wei, X., 2018. A cloud boundary detection scheme combined with aslic and cnn using zy-3, gf-1/2 satellite imagery. *The International Archives of the Photogrammetry, Remote Sensing and Spatial Information Sciences*, 42, 455-458.
- Hasan, A., Witharana, C., Udawalpola, M. R., Liljedahl, A. K., 2022. Detection of Clouds in Medium-Resolution Satellite Imagery Using Deep Convolutional Neural Nets. *The International Archives of the Photogrammetry, Remote Sensing and Spatial Information Sciences*, 46, 103-109.
- Kim, S. H., Eun, J., 2021. Development of Cloud and Shadow Detection Algorithm for Periodic Composite of Sentinel-2A/B Satellite Images. *Korean Journal of Remote Sensing*, 37(5\_1), 989-998.
- Lee, H. S., Lee, K. S., 2015. Development of cloud detection method with Geostationary Ocean Color Imagery for land applications. *Korean Journal of Remote Sensing*, 31(5), 371-384.
- Lyapustin, A., Wang, Y., Frey, R., 2008. An automatic cloud mask algorithm based on time series of MODIS measurements. *Journal of Geophysical Research: Atmospheres*, 113(D16).
- Sisodia, P. S., Tiwari, V., Kumar, A., 2014. Analysis of supervised maximum likelihood classification for remote sensing image. In *International conference on recent advances and innovations in engineering (ICRAIE-2014)*, 1-4.
- Zack, G. W., Rogers, W. E., Latt, S. A., 1977. Automatic measurement of sister chromatid exchange frequency. *Journal of Histochemistry & Cytochemistry*, 25(7), 741-753.

Zhong, B., Chen, W., Wu, S., Hu, L., Luo, X., Liu, Q., 2017. A cloud detection method based on relationship between objects of cloud and cloud-shadow for Chinese moderate to high resolution satellite imagery. *IEEE Journal of Selected Topics in Applied Earth Observations and Remote Sensing*, 10(11), 4898-4908.